JPET Fast Forward. Published on April 23, 2020 as DOI: 10.1124/jpet.119.263566
This article has not been copyedited and formatted. The final version may differ from this version.

Use of a non-invasive brain penetrating peptide-drug conjugate strategy to improve the delivery of opioid pain relief medications to the brain

Émilie Eiselt[1], Valérie Otis[1], Karine Belleville[1], Gaoqiang Yang[2], Alain Larocque[2], Anthony Régina[2], Michel Demeule[2], Philippe Sarret[1,3]* and Louis Gendron[1,3]*

[1] Département de pharmacologie-physiologie, Institut de pharmacologie de Sherbrooke, Centre de Recherche du Centre Hospitalier Universitaire de Sherbrooke, Faculté de médecine et des sciences de la santé, Université de Sherbrooke, Sherbrooke, Québec, Canada

[2] Angiochem Inc., Westmount, Québec, Montréal, QC, Canada H2X 3Y7

[3] Quebec Pain Research Network

***Corresponding authors**

Louis Gendron, Ph.D.
Department of Pharmacology-Physiology
Faculty of Medicine and Health Sciences
Université de Sherbrooke
3001, 12th Avenue North
Sherbrooke, Québec, J1H 5N4
Canada
Email: Louis.Gendron@USherbrooke.ca

Philippe Sarret, Ph.D.
Department of Pharmacology-Physiology
Faculty of Medicine and Health Sciences
Université de Sherbrooke
3001, 12th Avenue North
Sherbrooke, Québec, J1H 5N4
Canada
Email: Philippe.Sarret@USherbrooke.ca

Number of words in Abstract: 191
Number of words in the introduction: 643
Number of words in the discussion: 1489

Abbreviations: An2, Angiopep-2 peptide; BBB, blood-brain-barrier; LRP1, Low density lipoprotein receptor-related protein 1; M6G, morphine-3-glucuronide; M6G, morphine-6-glucuronide; MOP, mu opioid receptor; MPE, maximal antinociceptive effect; P-gp, P-glycoprotein

JPET Fast Forward. Published on April 23, 2020 as DOI: 10.1124/jpet.119.263566
This article has not been copyedited and formatted. The final version may differ from this version.

RUNNING TITLE

An2-morphine and An2-M6G conjugates as potent analgesics

ABSTRACT

The analgesic potency of morphine-6-glucuronide (M6G) has been shown to be 50-fold higher than morphine after intracerebral injection. However, the brain penetration of M6G is significantly lower than morphine, thus limiting its usefulness in pain management. Here, we created new entities by the conjugation of the Angiopep-2 peptide (An2) that crosses the blood-brain-barrier (BBB) by LRP1 receptor-mediated transcytosis, with either morphine or M6G. We demonstrated improvement of BBB permeability of these new entities compared with that of unconjugated M6G and morphine. Intravenous or subcutaneous administration of the An2-M6G conjugate exerted greater and more sustained analgesic activity than equivalent doses of either morphine or M6G. Likewise, subcutaneous An2-morphine induced a delayed but prolonged antinociceptive effect. The effects of these conjugates on the gastrointestinal tract motility were also evaluated. An2-morphine significantly reduced the intestinal transit time while An2-M6G exhibited a reduced constipation profile, as compared to an equimolar dose of morphine. In summary, we have developed new brain-penetrant opioid conjugates exhibiting improved analgesia to side-effect ratios. These results thus support the use of An2 carrier peptides as an innovative BBB targeting technology to deliver effective drugs such as M6G for the pain management.

Significance Statement

The metabolite M6G does not cross efficiently the blood-brain barrier. The LRP1 peptide ligand Angiopep-2 may serve as an effective drug delivery system to the brain. Here, we demonstrated that the coupling of M6G to An2 improves its brain penetration and significantly increases its analgesic potency. The An2-M6G conjugate has a favorable side-effect profile that includes reduction of developing constipation. An2-M6G exhibits a unique pharmacodynamic profile with a better therapeutic window than morphine.

INTRODUCTION

Despite important research efforts, the relief of moderate to severe pain still relies on opioids. Indeed, since 1986 the World Health Organization (WHO) identifies morphine as the most suitable drug for the management of moderate to severe pain (Mercadante and Fulfaro, 2005). In addition to inducing profound analgesia, opioids are well-known to interfere with numerous physiological functions. At the peripheral level, most commonly used opioids, including morphine, activate the mu opioid receptor (MOP) in the gut, thus producing constipation, one of the main adverse effects of opioids (Bhimji and Whitten, 2018). Although morphine produces potent analgesia, high systemic doses are also needed due to the development of tolerance and its limited brain penetration, thus further increasing the incidence of adverse events (Oldendorf et al., 1972). Improving morphine and derivatives to cross the blood-brain barrier (BBB) could thus be key to increasing analgesia while reducing the peripheral adverse effects.

Previous studies have established the mechanism of action for morphine as well as its metabolism and disposition (De Gregori et al., 2012; Sverrisdóttir et al., 2015). Morphine is rapidly metabolized in the liver by the UDP-glucuronosyltransferase (UGT) enzyme. The major metabolite of morphine is morphine-3-glucuronide (M3G), while a smaller portion is converted to morphine-6-glucoronide (M6G) (De Gregori et al., 2012). After oral administration in human, the ratio of each metabolite to morphine is 9:1 and 50:1 respectively for M6G and M3G (Osborne et al., 1990). The addition of a glucuronide significantly increases the polarity of morphine and therefore facilitates its excretion in urine. In general, a single subcutaneous dose of morphine is excreted at 85% after 24h, with 75% in glucuronidated forms and only 10% in the non-metabolized form (Yeh, 1975). It has been shown that these two morphine metabolites differ profoundly in the management of pain. Several studies strongly suggest that M3G is a physiological antagonist for the analgesic effect of morphine (Andersen et al., 2003;

Shimomura et al., 1971). Although the exact mechanisms remain unclear, M3G is thought to be largely responsible for the phenomenon of morphine-induced hyperalgesia (Due et al., 2012; Roeckel et al., 2017; Shavit et al., 2005; Smith, 2000). In addition, there is evidence to support the role of M3G in the development of morphine tolerance (Lipkowski et al., 1994; Smith and Smith, 1995). Conversely, M6G exhibits a high analgesic potency (typically more than 50-fold that of morphine) following direct administration into the cerebral ventricles (i.c.v. injection), thus bypassing the BBB (Pasternak and Pan, 2013). Despite their high polarity and their low expected lipophilicity, multiple evidence suggest that M3G and M6G can barely cross the BBB (Carrupt et al., 1991; Smith, 2000; Yoshimura et al., 1973). Accordingly, the BBB penetration of morphine is approximately 30 to 50 times higher than that of M6G (Bickel et al., 1996; Wu et al., 1997). On the other hand, the passive transport of morphine across the BBB and/or its transporter-facilitated (active) passage have not yet been completely elucidated. However, various strategies have been proposed to improve the brain uptake of therapeutic agents, including delivery through active transporters or receptor-mediated transcytosis (Banks, 2016; Bertrand et al., 2010; Régina et al., 2008).

Given the high analgesic potency of M6G, without induction of the M3G metabolite that antagonizes the analgesic effect of morphine, M6G could be a promising drug to treat moderate to severe pain. The major issue of systemic use of M6G is its poor BBB permeability. In this study, we proposed to increase the BBB penetration of M6G and morphine by conjugation to the shuttle Angiopep-2 (An2). We have previously shown the advantage of An2 coupling in terms of improving brain delivery to treat pain (Demeule et al., 2007, 2014; Eiselt et al., 2019). Here, we thus investigated the potential therapeutic benefits of An2-morphine and An2-M6G after systemic administration in a rodent model of nociception as well as on the motility of the gastrointestinal tract.

MATERIALS AND METHODS

Compounds synthesis and conjugation

M6G (**4**) was prepared as described elsewhere.(Lacy and Sainsbury, 1995; Rukhman et al., 2001) N-succinimidyl-3-(2-pyridyldithio)propionate (SPDP) was purchased from TRC, Toronto. All other reagents and anhydrous solvents were purchased from Sigma-Aldrich (St. Louis, MO) and used as received. NMR (^{1}H, ^{13}C) spectra were recorded on Varian AS600 spectrometers (Palo Alto, CA, USA) in $CDCl_3$, CD_3OD, or DMSO with solvent resonance as the internal standard. Low- and high-resolution mass spectra were recorded on Bruker microTOF spectrometers (Billerica, MA, USA) using electron spray ionization (ESI-TOF). The purity of the conjugate target compounds was determined to be >95% by UPLC/MS on a Waters Acquity UPLC spectrometer (Milford MA, USA) and by HPLC on a Shimadzu SCL-10A HPLC (Columbia, MD, USA). UPLC was conducted on an Acquity UPLC BEH phenyl 1.7 µm column (2.1 mm x 50 mm) using a gradient of 10–90% MeCN-water (0.1% FA) at 0.5 mL/minute. HPLC was conducted on a Taxsil column 3 µm (4.6 mm x 50 mm) using a gradient of 10–70% MeCN-water (0.05% TFA) at 1 mL/minute. Analytical thin-layer chromatography was performed on Merck 60F 254 precoated silica gel plates. Flash column chromatography was performed on a Biotage system (Charlottesville, VA, USA) using Silicycle siliaflash cartridges (230-400 mesh). Purifications were performed with a phenyl column on a Waters PrepLC 4000 system (Milford MA, USA).

2: PyBOP (0.52 g, 1.0 mmol) and DIEA (0.32 ml, 1.83 mmol) were added consecutively to a solution of morphine (**1**) (0.29 g, 1.0 mmol) and PEGdiacid (0.22 g, 1.0 mmol) in DMF (8 ml) at 0 ^{o}C (Figure 1). The mixture was stirred at room temperature for 4 hours, diluted with 1% TFA in water (10 ml) and water (20 ml) and then filtered. The filtrate was loaded to a 220 ml phenyl column (0 to 14% MeCN in H_2O + 0.1% TFA). The desired product **2** (0.25 g, 51%)

was obtained as a colorless powder after lyophilization. HRMS (ESI, MicrOTOF), m/z calcd. for $C_{25}H_{31}NO_9$ 489.1999, found 490.1976 (M+1) (**Scheme 1**).

3: TBTU (0.17 g, 0.52 mmol) and DIEA (0.18 ml, 1.0 mmol) were added consecutively to a solution of **2** (0.25 g, 0.51 mmol) in DMF (6 ml) at 0°C. The mixture was stirred at room temperature for 1 hour, then Angiopep-2 (An2; 0.39 g, 0.17 mmol) in DMSO (2 ml) and DMF (2 ml) were added. The mixture was stirred at room temperature for 1 hour. The solution was diluted with 1% TFA in water (10 ml) and water (50 ml). The crude solution was purified using 220 ml phenyl column (4 to 32% MeCN in H_2O + 0.1% TFA). The desired product **3** (251 mg, 40%) was obtained as a colorless powder after lyophilization. UPLC purity, 95%.

5: PyBOP (1.04 g, 2.0 mmol) and DIEA (0.63 ml, 3.62 mmol) were added consecutively to a solution of M6G (**4**) (1.01 g, 1.75 mmol) and cystamine (0.23 g, 2.02 mmol) in DMF (15 ml) at 0°C. The mixture was stirred for 30 min at 0°C, diluted with 1% TFA in water (10 ml) and water (150 ml) and then filtered. The filtrate was loaded to a 220 ml phenyl column (0 to 14% MeCN in H_2O + 0.1% TFA). The desired product **5** (0.8 g, 72%) was obtained as a colorless powder after lyophilization. UPLC purity was 98%. ^{1}HNMR (300 MHz, MeOD) δ (ppm) 8.02 (m, 1H), 6.49 (m, 2H), 5.80 (d, 1H, J = 9.8 Hz), 5.25 (d, 1H, J = 9.7 Hz), 5.05 (d, 1H, J = 6.1 Hz), 4.57 (d, 1H, J = 7.6 Hz), 4.37 (m, 1H), 4.07 (s, 1H), 3.68 (d, 1H, J = 9.1 Hz), 3.50-3.23 (m, 7H), 3.20-2.75 (m, 6H), 2.52 (t, 2H, J = 6.8 Hz), 2.22 (m, 1H), 2.0 (m, 1H); ^{13}C NMR (75 MHz, MeOD) δ (ppm) 175.75, 147.55, 141.85, 134.07, 130.10, 126.17, 123.61, 121.16, 118.80, 103.47, 89.33, 77.47, 76.50, 74.88, 73.80, 73.47, 62.44, 43.54, 43.10, 40.50, 35.26, 24.40. HRMS (ESI, MicrOTOF), m/z calcd. for $C_{25}H_{32}N_2O_8S$ 520.1879, found 521.1835 (M+1).

6: SPDP (0.8 g, 2.55 mmol) and DIEA (0.44 ml, 2.55 mmol) were added consecutively to a solution of An2 (**3**) (1.88 g, 0.64 mmol) in DMSO (2.5 ml) and DMF (6 ml). The mixture was stirred at room temperature for 2 h, diluted with 0.1% TFA in water (20 ml) and water (50 ml). The crude solution was purified using 220 ml phenyl column (15 to 60% MeCN in H_2O + 0.1%

FA). The desired product **6** (1.11 g, 60%) was obtained as a colorless powder after lyophilization. UPLC purity, 95%. LC-HRMS (ESI, micrOTOF), m/z, calcd. for $C_{128}H_{170}N_{32}O_{34}S_6$ 2892.0915, found 1447.5050 (2+), 965.3478 (3+), 724.0177 (4+).

7: A mixture of **5** (0.5 g, 0.79 mmol), **6** (0.63 g, 0.22 mmol) and $NaHCO_3$ (94 mg, 1.08 mmol) in DMSO (10 ml) was stirred at room temperature for 30 min. The solution was cooled to 0°C, diluted with 1% TFA in water (10 ml) and water (80 ml). The crude solution was purified using 220 ml phenyl column (4 to 32% MeCN in H_2O + 0.1% TFA). The desired product **7** (630 mg, 70%) was obtained as a colorless powder after lyophilization. UPLC purity, 95%. LC-HRMS (ESI, micrOTOF), m/z, calcd. for $C_{188}H_{251}N_{35}O_{58}S_6$ 4120.6159, found 2061.7995 (2+), 1374.5352 (3+), 1031.1606 (4+).

Animals

Adult male Crl:CD-1 or C57BL/6 mice or adult male Sprague-Dawley rats (225-250 gr; 12-hour light/12-hour dark cycle; Charles River Laboratories, St-Constant, QC, Canada) were allowed ad libitum access to food and water. Rodents were acclimatized for 1 day to manipulations and devices prior to the behavioral studies, which were performed in a quiet room by the same experimenter between 8:00 AM and 12:00 AM. The experimental procedures in this study were approved by the Animal Care Committee of the University of Sherbrooke and were in accordance with policies and directives of the Canadian Council on Animal Care and adhere to the ARRIVE guidelines.

Brain uptake

Transcytosis of [^{125}I]-An2-morphine and [^{125}I]-An2-M6G into the brain was performed on adult male mice using the brain perfusion method and compared to [^{3}H]-morphine (Dagenais et al., 2000). Radiolabeled molecules were solubilized in a Krebs/bicarbonate buffer (128 mM NaCl,

24 mM $NaHCO_3$, 4.2 mM KCl, 2.4 mM NaH_2PO_4, 1.5 mM $CaCl_2$, 0.9 mM $MgCl_2$, and 9 mM *D*-glucose; gassed with 95% O_2 and 5% CO_2, pH 7.4, 37°C) and loaded on the infusion pump (Harvard pump PHD 2000 ; Harvard Apparatus) connected to a catheter beforehand inserted into the right carotid as previously described (Demeule et al., 2014). The radiolabeled compounds at 1 μM were perfused into the carotid under 5 minutes for the time course brain uptake or 2 minutes for the quantification in separate fractions at a flow rate of 2.5 mL/min, followed by a 30-second Krebs buffer perfusion. Right brain hemisphere was then quickly isolated on ice after mice euthanasia followed by various purification steps, as described precisely by Demeule et al, 2014. Samples were placed in 5 mL glass tubes, and the radioactivity was determined using a Wizard^2 Automatic Gamma Counter. Total brain homogenate data are represented as apparent V_d by a least-squares regression.

For capillary depletion, the mouse brain was homogenized on ice in Ringer's HEPES buffer with 0.1% BSA in a glass homogenizer. Brain homogenate was then mixed thoroughly with 35% Dextran 70 (50:50) and centrifuged at 5,400 *g* for 10 minutes at 4°C. The supernatant (brain parenchyma) and the pellet (capillaries) were separated. Aliquots of homogenates, supernatants, pellets, and perfusates were collected at every step to determine the concentration of each radiolabeled compound necessary for the calculation of the apparent V_d in the different brain fractions. Data are expressed as the mean ± SEM (n= 4) and were analyzed using GraphPad Prism 7.0.

Acute pain models

The antinociceptive effects of morphine, M6G, An2-morphine and An2-M6G have been assessed using different pain modalities, including hot-plate and heat tail-flick immersion tests. In the hot-plate assay, male CD1 mice (25–30 g) were placed onto a metal plate heated at 54°C surrounded by a Plexiglas cylinder (d x h: 13 cm × 19 cm). Baseline readings were done for

each mouse immediately prior to drug injection. Animal latency to the first foot-lick was recorded (maximum 30 seconds, to prevent tissue damage). The analgesic potencies of morphine, M6G, An2-morphine and An2-M6G were also evaluated in adult male Sprague-Dawley rats using the tail flick test. This acute pain test consists of measuring the time taken to flick or withdraw the tail from the heat after immersion of 5 cm of the tail in a hot water bath (53°C +/- 0.5°C). Before administrating the compounds, baselines are measured 3 times within 30 minutes. Rats are then tested every 15-30 minutes up to 6 hours following drug administration (*i.v.* or *s.c.*). A cut-off of 10 seconds was imposed for the duration of the test to avoid tissue damage. Hot-plate and tail-flick latencies were used to determine the percentage of the maximum possible effect (%MPE) calculated as %MPE = 100 X (Time to tail withdrawal – baseline) / (cut off – baseline). The Area Under the Curve (AUC) was also determined to evaluate the total antinociceptive effect of each compound.

Charcoal meal test

Constipation has been assessed by measuring the gastrointestinal tract motility using the charcoal meal test. Food deprived (16 h) rats are injected *s.c.* with saline, morphine, M6G, An2-morphine, or An2-M6G. 30 minutes after drug injection, 2 mL of a charcoal meal solution (5% arabic gum and 10% charcoal in water) is administered to the rats by gavage. The animals are euthanized exactly 60 minutes after drug injection and the progression of the charcoal in the intestine is measured as a ratio of progression/total length of the intestine. The results are presented as a percentage of progression of the charcoal meal in the intestine.

Statistical analysis

Two-way ANOVA and Tukey's multiple comparison post-hoc test was used to compare the brain uptake of radiolabeled compounds. Data of hot-plate and tail-flick experiments were

compared using one-way ANOVA test followed by either Dunnett's or Tukey's multiple comparison test. Data of gastrointestinal tract motility experiments were compared using the Kruskal-Wallis nonparametric test followed by Dunn's multiple comparison test. Statistical analyses were performed using GraphPad Prism (version 7.00; GraphPad Software Inc.).

JPET Fast Forward. Published on April 23, 2020 as DOI: 10.1124/jpet.119.263566
This article has not been copyedited and formatted. The final version may differ from this version.

RESULTS

In vivo brain penetration

Morphine and M6G were first conjugated to the Angiopep-2 (An2), a 19-mer peptide that crosses the BBB by LRP1 receptor-mediated transcytosis. As described in the Methods section (**Scheme 1**), the new chemical entities carried three molecules of morphine or M6G per An2. The resulting new drug conjugates were then evaluated for their ability to penetrate the BBB (**Fig. 1**). Transcytosis of [^{125}I]-An2-morphine, [^{125}I]-An2-M6G and [^{3}H]-morphine over time was determined by *in situ* brain perfusion after intravenous (*i.v*) drug administration. As opposed to morphine (4.9 ± 2.7 mL/100 g of brain), the distribution volume (V_d) of [^{125}I]-An2-morphine and [^{125}I]-An2-M6G found in total brain homogenates increased linearly over time to respectively reach 60.6 ± 33 mL/100 g of brain and 221.1 ± 98 mL/100 g of brain after 4 minutes (**Fig. 1A**). The BBB influx rate constants (K*in*) of each compound, corresponding to the slope of the curves in Figure 1A, are shown in **Table 1**. The K*in* for the conjugate An2-morphine was found to be 12-fold higher ($2.7x10^{-3}$ mL/s/g) than that of the unconjugated morphine ($2.2x10^{-4}$ mL/s/g). Likewise, the conjugation of M6G to An2 improved its influx rate from blood to brain by more than 440-fold ($8.8x10^{-3}$ mL/s/g compared to the theoretical value of M6G which is $2x10^{-5}$ mL/s/g).(Wu et al., 1997b) The K*in* of An2-M6G is indeed similar to that of glucose ($9.5x10^{-3}$ mL/s/g) which was used as a positive control for brain permeability(Wu et al., 1997b). In order to confirm penetration of the compounds in the parenchyma compartment, a depletion of brain capillaries was then performed. We estimated apparent V_d of An2-morphine and An2-M6G after 2 minutes of perfusion in the total brain tissue, capillaries and parenchymal fraction (**Fig. 1B**). When compared to morphine, An2-morphine had a significantly higher V_d in the brain and parenchymal fractions. Likewise, An2-M6G was mainly found within the brain parenchyma. Overall 80-90% of An2-morphine and An2-M6G were associated with the parenchymal fraction and only 10-20% remained trapped within the brain vasculature. These

results demonstrate that both An2-morphine and An2-M6G were able to cross the BBB more efficiently than unconjugated opioids.

Antinociceptive effects of An2-morphine and An2-M6G following intravenous administration

Using the rat tail-flick test, we evaluated the antinociceptive effects of morphine, M6G, An2-morphine and An2-M6G after systemic delivery. Morphine and An2-morphine induced a dose- and time-dependent increase in the time reaction to tail withdrawal (**Fig. 2**). Our results show that the administration of morphine (0.3 – 3 mg/kg, *i.v.*) produced a maximal antinociceptive effect (%MPE) of 88.6% at the highest dose tested (**Fig. 2A-C**). When equimolar doses of morphine conjugated to An2 (An2-morphine; 3 mg/kg) were compared to unconjugated morphine (1 mg/kg) at the peak effect, similar levels of antinociception were observed, reaching 46% and 49.7% of MPE, respectively (**Fig. 2B and E**).

The analgesic effects of *i.v.* M6G and An2-M6G were also evaluated in the rat tail-flick assay (**Fig. 3**). These two compounds also produced a time- and dose-dependent antinociception. The *i.v.* injection of 1.5 to 4.5 mg/kg M6G induced a %MPE ranging from 30% to 87% (**Fig. 3A-C**). Most interestingly, An2-M6G induced a long-lasting, robust dose-dependent antinociceptive effect. Indeed, at an equimolar dose of 3 mg/kg of morphine (i.e. 12 mg/kg), An2-M6G produced a latency to tail withdrawal reaching the cutoff (i.e. 10 s) after 30 min, an effect lasting at least 3 hours (**Fig. 3D-F**). The %MPE calculated at 60 min following the *i.v.* injection of An2-M6G at 4, 8 and 12 mg/kg (equivalent to 1, 2 and 3 mg/kg of morphine and to 1.5, 3 and 4.5 mg/kg of M6G) was 34.9%, 66.2% and 100%, respectively (**Fig. 3E**).

Similar results were also obtained in the hot-plate test using male CD1 mice (**Fig. 4**). Over a 2-hour period, both morphine and An2-morphine caused similar increases in hot-plate latencies

(**Fig. 4A-C**). Likewise, mice receiving An2-M6G (6 mg/kg i.v.) also exhibited a sustained and superior analgesic effect compared to equimolar doses of either morphine or M6G (**Fig. 4D-F**).

Antinociceptive effects produced by the subcutaneous administration of An2-morphine and An2-M6G

We also measured the analgesic effect of An2-morphine and An2-M6G following *s.c.* injections (**Fig. 5**). Despite similar MPE at the peak effect, *s.c.* injection of 20 mg/kg An2-morphine (equivalent to 5.5 mg/kg of morphine) produced an analgesic effect that was more prolonged over the time than what was observed with an equimolar dose of morphine (**Fig. 5A-B**). indeed, when the area under the curve (AUC) was calculated for each compound, we found that the level of antinociception induced by An2-morphine over the course of 120 minutes was significantly higher than that of morphine (**Fig. 5C**). The antinociceptive effects of *s.c.* 12 mg/kg An2-M6G (representing an equimolar dose of 4.5 mg/kg M6G or 3 mg/kg morphine) were also determined (**Fig. 5D-F**). The duration of antinociception was different for each of the compounds. Indeed, the antinociceptive effects of 3 mg/kg morphine returned to baseline after 90 minutes while the antinociceptive effects of 4.5 mg/kg M6G returned to baseline only after 180 minutes. Most interestingly, the antinociceptive properties of the An2-M6G conjugate were maintained for over 380 minutes (**Fig. 5D**). The AUC were calculated for each compound and included only the first 180 minutes following the injections (**Fig. 5D**). The AUC for M6G and An2-M6G were found to be significantly higher than both saline and morphine groups. Furthermore, the antinociception produced by An2-M6G was significantly higher than that of an equimolar dose of M6G (**Fig. 5F**).

Modulation of the gastrointestinal tract motility

JPET Fast Forward. Published on April 23, 2020 as DOI: 10.1124/jpet.119.263566
This article has not been copyedited and formatted. The final version may differ from this version.

In order to evaluate if An2-morphine and An2-M6G produced constipation, one of the main adverse effects of opioids, the effects of An2-morphine at 20 mg/kg (equimolar to 5.5 mg/kg of morphine) and An2-M6G at 4 and 20 mg/kg (respectively equimolar to 1 and 5 mg/kg of morphine) were measured and compared to morphine at 1, 5 and 10 mg/kg. As reported in **Table 2**, *s.c.* administration of morphine produced a dose-dependent decrease of the charcoal meal progression in the intestine of 58.0% ± 2.7%, 49.7% ± 2.7%, and 28.6% ± 3.7% at 1, 5 and 10 mg/kg of morphine, respectively, as compared to 73.4% ± 2.2% in the saline-treated group. An2-morphine at 20 mg/kg induced a similar decrease as morphine at an equimolar dose with a progression of 45.1% ± 5.1%. Interestingly, the An2-M6G doses did not produced a significant decrease of the gastrointestinal tract motility when compared to the saline group. A dose of 4 mg/kg induced 61.5% ± 3.3% of charcoal meal progression and 20 mg/kg induced 59.7% ± 3.1% (respectively equimolar to 1 and 5 mg/kg of morphine), suggesting that in addition to its higher antinociceptive action, An2-M6G produced minimal effects on the gastrointestinal tract motility.

DISCUSSION

Despite its important adverse effects, morphine remains one of the most commonly used analgesics for the treatment of moderate to severe pain (Balch and Trescot, 2010). Among all adverse effects produced by morphine, constipation is often the most debilitating for patients. Importantly, constipation is not significantly subject to tolerance and is therefore amplified as the doses escalate to compensate for analgesic tolerance. While the analgesic effects of opioids are mainly mediated by central receptors, constipation is due to a direct action on the gastrointestinal (GI) tract (Holzer, 2009). However, the ability of morphine to cross the BBB is limited and it is estimated that only about 0.02% of the total amount of morphine reach the brain following systemic administration (Banks and Kastin, 1994; Oldendorf et al., 1972). Due to this poor BBB permeability, high doses of morphine are needed to produce analgesia, thus increasing the adverse effects (Koyyalagunta, 2007; Oldendorf et al., 1972). The second main problem of morphine therapy is the high interindividual variability in serum concentrations of morphine and its metabolites M6G and M3G among patients (Klepstad et al., 2003). Indeed, the level of glucuronidation of morphine in M6G and M3G by the glucuronosyltransferase enzyme, UGT2B7 can significantly impact the amplitude of morphine antinociception (Yang et al., 2017). Accordingly, it has been reported in daily clinical practices that patients with diverse UGT2B7 gene polymorphisms have a different analgesic response to the same dose of morphine (Bastami et al., 2014).

In this study, we created new brain-penetrating peptide drug conjugates to increase the BBB permeability of morphine and its highly potent metabolite M6G. We hypothesized that such an approach could ameliorate the therapeutic profiles of morphine and M6G by increasing their brain distribution and therefore reducing the dose required to produce analgesia. Here, we conjugated morphine and M6G to the brain penetrant 19-mer peptide An2. The An2 peptide was previously shown to efficiently bind to the LDL receptor-related protein-1 (LRP1) present

at the luminal endothelial cells of brain capillaries (Demeule et al., 2007). Using LRP1 receptors, the An2-drug complex can therefore cross the BBB via a receptor-mediated transcytosis mechanism (Bertrand et al., 2010; Demeule et al., 2007). This approach was successfully applied to improve brain uptake of peptides like neurotensin or anticancer agents, such as the paclitaxel, doxorubicin or etoposide (Bertrand et al., 2011; Demeule et al., 2007, 2014; Eiselt et al., 2019; Régina et al., 2008; Thomas et al., 2009). In order to achieve optimal brain concentrations of morphine and M6G, these opioid drugs were conjugated with a ratio of 3 to 1 to the An2 peptide. As expected, such a coupling strategy produced a significant increase in the parenchymal uptake of morphine and M6G. It was previously shown that the brain penetration of M6G is more than 30 to 50 fold lower than that of morphine (Bickel et al., 1996; Wu et al., 1997b). However, when coupled to An2, the brain penetration of M6G injected intravenously was 3-fold and 40-fold higher than that of An2-morphine and non-conjugated morphine, respectively. The level of BBB permeability of An2-M6G can indeed be compared to the permeability of glucose (McAllister et al., 2001).

According to the literature, M6G is a strong mu opioid receptor agonist with even higher affinity than morphine itself (Chen et al., 1991). Importantly, previous studies revealed that about 96.6%, 85.6%, and 85.4% of the analgesic effect of oral, *s.c.* and *i.v.* of morphine is caused by M6G (Klimas and Mikus, 2014). Although the coupling of morphine to An2 had no major effects on its antinociceptive properties following its *i.v.* administration, its *s.c.* delivery was found to produce a delayed but prolonged antinociception, up to 2 hours, compared to equimolar dose of unconjugated morphine. As previously shown, despite a low brain penetration, we observed that *i.v.* or *s.c.* M6G produced a dose- and time-dependent antinociceptive effect in the rat tail-flick assay similar to that of morphine (Paul et al., 1989). Our results further demonstrated that the An2-M6G conjugate was notably more potent than unconjugated M6G, with all animals reaching the cutoff 30 minutes after *i.v.* injection of 12 mg/kg An2-M6G

(which is equivalent to 3 mg/kg of morphine and to 4.5 mg/kg of M6G). More importantly, *i.v* An2-M6G has also a longer duration of action when compared to equimolar doses of morphine and M6G. Indeed, the antinociceptive effect of 12 mg/kg of An2-M6G remained maximal after 3 hours while the latency to tail withdrawal was back to the baseline 120 minutes after *i.v.* injection of either morphine or M6G. Similarly, the analgesic profile of *i.v.* An2-M6G was superior to that of M6G and morphine in CD1 mice submitted to the hot-plate test. Finally, *s.c.* delivery of An2-M6G produced long-lasting analgesia with greater potency and efficacy than unconjugated M6G and morphine. These observations support the hypothesis that a significantly higher level of M6G penetrates into the brain when conjugated to An2 and highlights the potential use of lower doses of opioids to provide effective antinociception. Accordingly, brain penetration of M6G is mandatory to produce antinociception since naloxone, but not naloxone methiodide (which does not enter brain from blood), was shown to block the analgesic effect of M6G (Wu et al., 1997b). Despite similar pharmacokinetic properties, M6G and morphine differ in their lipid solubility. M6G was reported to have a 200-fold lower lipid solubility than morphine (Wu et al., 1997b). The increased polarity of the glucuronide metabolite M6G also limits its diffusion through biological membranes (Milne et al., 1997). Hence, in order to cross the BBB, M6G was shown to use the GLUT1 transporters, albeit with a weak capacity. As opposed to morphine, M6G was, however, shown to be a poor P-glycoprotein (P-gp) substrate which might explain its longer duration of effect as well as its higher potency when it reaches the brain (Bourasset et al., 2003).

When administrated to patients, morphine also produces a number of unwanted and debilitating effects, including constipation, nausea, respiratory depression, drowsiness, and tolerance (Benyamin et al., 2008). Interestingly, previous studies suggest that M6G is devoid of or exhibits less adverse effects than morphine. For instance, in a randomized doubled-blind study of patients undergoing major joint replacement, M6G showed a higher analgesic potency with

less respiratory suppression and somnolence, compared with morphine (Hanna et al., 2005; Penson et al., 2000). Furthermore, in a study with healthy volunteers, the frequency of nausea, itching and rash after M6G was significantly reduced compared to morphine (Hanna et al., 1991). M6G was also found devoid of nausea, vomiting, and sedation in cancer patients (Osborne et al., 1992). Finally, a study by Cann et al. in which 144 women received either M6G or morphine as part of general anesthesia for day-case surgery revealed that M6G has a better safety profile than morphine (Cann et al., 2002). In order to see whether or not a parallel decrease in the unwanted effect of An2-M6G could be observed, we compared the effect of An2-M6G on the gastrointestinal tract motility to that of morphine and M6G. Using the charcoal meal test, we found that conjugation of morphine to An2 does not prevent the effect on the gastrointestinal tract. Indeed, at equivalent dose of morphine, An2-morphine significantly reduced the gastrointestinal transit of the charcoal meal. By contrast, An2-M6G, even at 20 mg/kg (equivalent to 5 mg/kg of morphine) did not significantly reduced the motility of the gastrointestinal tract. This is of a particular interest as this dose of An2-M6G produced a maximal and sustained antinociception effect in the acute pain test, further supporting that improving the BBB penetration of opioids has the potential to improve their therapeutic profile. The conjugation of M6G or morphine to An2 may also offer additional benefits, such as reduction of analgesic tolerance. Indeed, previous studies support the idea that the development of morphine tolerance is partly due to an increase in the expression level of the drug transporter, P-gp which decreases the morphine brain concentration (Ochiai et al., 2016). Accordingly, the brain uptake and the analgesic effect of morphine are increased in P-gp knockout mice (Hamabe et al., 2006, 2007). Consequently, the active transport of An2-M6G or An2-morphine by LRP1 receptor-mediated transcytosis may limit the development of tolerance.

JPET Fast Forward. Published on April 23, 2020 as DOI: 10.1124/jpet.119.263566
This article has not been copyedited and formatted. The final version may differ from this version.

In conclusion, our results demonstrate that the conjugation of M6G with BBB penetrating peptides such as An2 presents many advantages over the use of morphine: (1) improvement of the brain penetration of M6G results in a significant increase in its analgesic potency as well as duration of antinociceptive action; (2) a more favorable side-effect profile that includes reduction of the risk of developing constipation, when compared with morphine; (3) elimination of the interindividual variability in morphine analgesic response, and finally (4) prevention of the adverse effects associated with the accumulation of the major metabolite of morphine (i.e. M3G). Altogether, these results indicate that the An2-M6G conjugate exhibits a unique pharmacodynamic profile with a better therapeutic window than morphine, which make it an attractive option for developing pain-relieving medications.

Author contributions

Participated in research design: Gendron, Sarret and Demeule

Conducted experiments: Otis, Belleville, Yang, Larocque and Régina

Performed data analysis: Eiselt

Wrote or contributed to the writing of the manuscript: Eiselt, Gendron and Sarret with the contributions of all authors.

References:

Andersen, G., Christrup, L., and Sjøgren, P. (2003). Relationships among morphine metabolism, pain and side effects during long-term treatment: an update. J. Pain Symptom Manage. *25*, 74–91.

Balch, R.J., and Trescot, A. (2010). Extended-release morphine sulfate in treatment of severe acute and chronic pain. J. Pain Res. *3*, 191–200.

Banks, W.A. (2016). From blood-brain barrier to blood-brain interface: new opportunities for CNS drug delivery. Nat. Rev. Drug Discov. *15*, 275–292.

Banks, W.A., and Kastin, A.J. (1994). Opposite direction of transport across the blood-brain barrier for Tyr-MIF-1 and MIF-1: comparison with morphine. Peptides *15*, 23–29.

Bastami, S., Gupta, A., Zackrisson, A.-L., Ahlner, J., Osman, A., and Uppugunduri, S. (2014). Influence of UGT2B7, OPRM1 and ABCB1 gene polymorphisms on postoperative morphine consumption. Basic Clin. Pharmacol. Toxicol. *115*, 423–431.

Benyamin, R., Trescot, A.M., Datta, S., Buenaventura, R., Adlaka, R., Sehgal, N., Glaser, S.E., and Vallejo, R. (2008). Opioid complications and side effects. Pain Physician *11*, S105-120.

Bertrand, Y., Currie, J.-C., Demeule, M., Régina, A., Ché, C., Abulrob, A., Fatehi, D., Sartelet, H., Gabathuler, R., Castaigne, J.-P., Stanimirovic, D., and Béliveau, R. (2010). Transport characteristics of a novel peptide platform for CNS therapeutics. J. Cell. Mol. Med. *14*, 2827–2839.

Bertrand, Y., Currie, J.-C., Poirier, J., Demeule, M., Abulrob, A., Fatehi, D., Stanimirovic, D., Sartelet, H., Castaigne, J.-P., and Béliveau, R. (2011). Influence of glioma tumour microenvironment on the transport of ANG1005 via low-density lipoprotein receptor-related protein 1. Br. J. Cancer *105*, 1697–1707.

Bhimji, S.S., and Whitten, R. (2018). Constipation, Opioid Induced. In StatPearls, (Treasure Island (FL): StatPearls Publishing), p.

Bickel, U., Schumacher, O.P., Kang, Y.S., and Voigt, K. (1996). Poor permeability of morphine 3-glucuronide and morphine 6-glucuronide through the blood-brain barrier in the rat. J. Pharmacol. Exp. Ther. *278*, 107–113.

Bourasset, F., Cisternino, S., Temsamani, J., and Scherrmann, J.-M. (2003). Evidence for an active transport of morphine-6-beta-d-glucuronide but not P-glycoprotein-mediated at the blood-brain barrier. J. Neurochem. *86*, 1564–1567.

Cann, C., Curran, J., Milner, T., and Ho, B. (2002). Unwanted effects of morphine-6-glucoronide and morphine. Anaesthesia *57*, 1200–1203.

Carrupt, P.A., Testa, B., Bechalany, A., el Tayar, N., Descas, P., and Perrissoud, D. (1991). Morphine 6-glucuronide and morphine 3-glucuronide as molecular chameleons with unexpected lipophilicity. J. Med. Chem. *34*, 1272–1275.

Chen, Z.R., Irvine, R.J., Somogyi, A.A., and Bochner, F. (1991). Mu receptor binding of some commonly used opioids and their metabolites. Life Sci. *48*, 2165–2171.

Dagenais, C., Rousselle, C., Pollack, G.M., and Scherrmann, J.M. (2000). Development of an in situ mouse brain perfusion model and its application to mdr1a P-glycoprotein-deficient mice. J. Cereb. Blood Flow Metab. Off. J. Int. Soc. Cereb. Blood Flow Metab. *20*, 381–386.

De Gregori, S., De Gregori, M., Ranzani, G.N., Allegri, M., Minella, C., and Regazzi, M. (2012). Morphine metabolism, transport and brain disposition. Metab. Brain Dis. *27*, 1–5.

Demeule, M., Regina, A., Che, C., Poirier, J., Nguyen, T., Gabathuler, R., Castaigne, J.-P., and Beliveau, R. (2007). Identification and Design of Peptides as a New Drug Delivery System for the Brain. J. Pharmacol. Exp. Ther. *324*, 1064–1072.

Demeule, M., Beaudet, N., Régina, A., Besserer-Offroy, É., Murza, A., Tétreault, P., Belleville, K., Ché, C., Larocque, A., Thiot, C., Béliveau, R., Longpré, J.-M., Marsault, E., Leduc, R., Lachowicz, J.E., Gonias, S.L., Castaigne, J.-P., and Sarret, P. (2014). Conjugation of a brain-penetrant peptide with neurotensin provides antinociceptive properties. J. Clin. Invest. *124*, 1199–1213.

Due, M.R., Piekarz, A.D., Wilson, N., Feldman, P., Ripsch, M.S., Chavez, S., Yin, H., Khanna, R., and White, F.A. (2012). Neuroexcitatory effects of morphine-3-glucuronide are dependent on Toll-like receptor 4 signaling. J. Neuroinflammation *9*, 200.

Eiselt, E., Côté, J., Longpré, J.-M., Blais, V., Sarret, P., and Gendron, L. (2019). The combination of opioid and neurotensin receptor agonists improves their analgesic/adverse effect ratio. Eur. J. Pharmacol. *848*, 80–87.

Hamabe, W., Maeda, T., Fukazawa, Y., Kumamoto, K., Shang, L.Q., Yamamoto, A., Yamamoto, C., Tokuyama, S., and Kishioka, S. (2006). P-glycoprotein ATPase activating effect of opioid analgesics and their P-glycoprotein-dependent antinociception in mice. Pharmacol. Biochem. Behav. *85*, 629–636.

Hamabe, W., Maeda, T., Kiguchi, N., Yamamoto, C., Tokuyama, S., and Kishioka, S. (2007). Negative relationship between morphine analgesia and P-glycoprotein expression levels in the brain. J. Pharmacol. Sci. *105*, 353–360.

Hanna, M.H., Peat, S.J., Knibb, A.A., and Fung, C. (1991). Disposition of morphine-6-glucuronide and morphine in healthy volunteers. Br. J. Anaesth. *66*, 103–107.

Hanna, M.H., Elliott, K.M., and Fung, M. (2005). Randomized, double-blind study of the analgesic efficacy of morphine-6-glucuronide versus morphine sulfate for postoperative pain in major surgery. Anesthesiology *102*, 815–821.

Holzer, P. (2009). Opioid receptors in the gastrointestinal tract. Regul. Pept. *155*, 11–17.

Klepstad, P., Dale, O., Kaasa, S., Zahlsen, K., Aamo, T., Fayers, P., and Borchgrevink, P.C. (2003). Influences on serum concentrations of morphine, M6G and M3G during routine clinical drug monitoring: a prospective survey in 300 adult cancer patients. Acta Anaesthesiol. Scand. *47*, 725–731.

Klimas, R., and Mikus, G. (2014). Morphine-6-glucuronide is responsible for the analgesic effect after morphine administration: a quantitative review of morphine, morphine-6-glucuronide, and morphine-3-glucuronide. Br. J. Anaesth. *113*, 935–944.

Koyyalagunta, D. (2007). chapter 113 - Opioid Analgesics. In Pain Management, S.D. Waldman, and J.I. Bloch, eds. (Philadelphia: W.B. Saunders), pp. 939–964.

Lacy, C., and Sainsbury, M. (1995). A synthesis of morphine-6-glucuronide. Tetrahedron Lett. *36*, 3949–3950.

Lipkowski, A.W., Carr, D.B., Langlade, A., Osgood, P.F., and Szyfelbein, S.K. (1994). Morphine-3-glucuronide: silent regulator of morphine actions. Life Sci. *55*, 149–154.

McAllister, M.S., Krizanac-Bengez, L., Macchia, F., Naftalin, R.J., Pedley, K.C., Mayberg, M.R., Marroni, M., Leaman, S., Stanness, K.A., and Janigro, D. (2001). Mechanisms of glucose transport at the blood-brain barrier: an in vitro study. Brain Res. *904*, 20–30.

Mercadante, S., and Fulfaro, F. (2005). World Health Organization guidelines for cancer pain: a reappraisal. Ann. Oncol. Off. J. Eur. Soc. Med. Oncol. *16 Suppl 4*, iv132-135.

Milne, R.W., Jensen, R.H., Larsen, C., Evans, A.M., and Nation, R.L. (1997). Comparison of the disposition of hepatically-generated morphine-3-glucuronide and morphine-6-glucuronide in isolated perfused liver from the guinea pig. Pharm. Res. *14*, 1014–1018.

Ochiai, W., Kaneta, M., Nagae, M., Yuzuhara, A., Li, X., Suzuki, H., Hanagata, M., Kitaoka, S., Suto, W., Kusunoki, Y., Kon, R., Miyashita, K., Masukawa, D., Ikarashi, N., Narita, M., Suzuki, T., and Sugiyama, K. (2016). Mice with neuropathic pain exhibit morphine tolerance due to a decrease in the morphine concentration in the brain. Eur. J. Pharm. Sci. Off. J. Eur. Fed. Pharm. Sci. *92*, 298–304.

Oldendorf, W.H., Hyman, S., Braun, L., and Oldendorf, S.Z. (1972). Blood-brain barrier: penetration of morphine, codeine, heroin, and methadone after carotid injection. Science *178*, 984–986.

Osborne, R., Joel, S., Trew, D., and Slevin, M. (1990). Morphine and metabolite behavior after different routes of morphine administration: demonstration of the importance of the active metabolite morphine-6-glucuronide. Clin. Pharmacol. Ther. *47*, 12–19.

Osborne, R., Thompson, P., Joel, S., Trew, D., Patel, N., and Slevin, M. (1992). The analgesic activity of morphine-6-glucuronide. Br. J. Clin. Pharmacol. *34*, 130–138.

Pasternak, G.W., and Pan, Y.-X. (2013). Mu Opioids and Their Receptors: Evolution of a Concept. Pharmacol. Rev. *65*, 1257–1317.

Paul, D., Standifer, K.M., Inturrisi, C.E., and Pasternak, G.W. (1989). Pharmacological characterization of morphine-6 beta-glucuronide, a very potent morphine metabolite. J. Pharmacol. Exp. Ther. *251*, 477–483.

Penson, R.T., Joel, S.P., Bakhshi, K., Clark, S.J., Langford, R.M., and Slevin, M.L. (2000). Randomized placebo-controlled trial of the activity of the morphine glucuronides. Clin. Pharmacol. Ther. *68*, 667–676.

Régina, A., Demeule, M., Ché, C., Lavallée, I., Poirier, J., Gabathuler, R., Béliveau, R., and Castaigne, J.-P. (2008). Antitumour activity of ANG1005, a conjugate between paclitaxel and the new brain delivery vector Angiopep-2. Br. J. Pharmacol. *155*, 185–197.

Roeckel, L.-A., Utard, V., Reiss, D., Mouheiche, J., Maurin, H., Robé, A., Audouard, E., Wood, J.N., Goumon, Y., Simonin, F., and Gaveriaux-Ruff, C. (2017). Morphine-induced hyperalgesia involves mu opioid receptors and the metabolite morphine-3-glucuronide. Sci. Rep. *7*, 10406.

Rukhman, I., Yudovich, L., Nisnevich, G., and Gutman, A.L. (2001). Selective synthesis of both isomers of morphine 6-β-d-glucuronide and their analogs. Tetrahedron *57*, 1083–1092.

Shavit, Y., Wolf, G., Goshen, I., Livshits, D., and Yirmiya, R. (2005). Interleukin-1 antagonizes morphine analgesia and underlies morphine tolerance. Pain *115*, 50–59.

Shimomura, K., Kamata, O., Ueki, S., Ida, S., Oguri, K., Yoshimura, H., and Tsukamoto, H. (1971). Analgesic effect of morphine glucuronides. Tohoku J. Exp. Med. *105*, 45–52.

Smith, M.T. (2000). Neuroexcitatory effects of morphine and hydromorphone: evidence implicating the 3-glucuronide metabolites. Clin. Exp. Pharmacol. Physiol. *27*, 524–528.

Smith, G.D., and Smith, M.T. (1995). Morphine-3-glucuronide: evidence to support its putative role in the development of tolerance to the antinociceptive effects of morphine in the rat. Pain *62*, 51–60.

Sverrisdóttir, E., Lund, T.M., Olesen, A.E., Drewes, A.M., Christrup, L.L., and Kreilgaard, M. (2015). A review of morphine and morphine-6-glucuronide's pharmacokinetic-pharmacodynamic relationships in experimental and clinical pain. Eur. J. Pharm. Sci. Off. J. Eur. Fed. Pharm. Sci. *74*, 45–62.

Thomas, F.C., Taskar, K., Rudraraju, V., Goda, S., Thorsheim, H.R., Gaasch, J.A., Mittapalli, R.K., Palmieri, D., Steeg, P.S., Lockman, P.R., and Smith, Q.R. (2009). Uptake of ANG1005, a novel paclitaxel derivative, through the blood-brain barrier into brain and experimental brain metastases of breast cancer. Pharm. Res. *26*, 2486–2494.

Wu, D., Kang, Y.S., Bickel, U., and Pardridge, W.M. (1997). Blood-brain barrier permeability to morphine-6-glucuronide is markedly reduced compared with morphine. Drug Metab. Dispos. Biol. Fate Chem. *25*, 768–771.

Yang, Z.-Z., Li, L., Wang, L., Yuan, L.-M., Xu, M.-C., Gu, J.-K., Jiang, H., Yu, L.-S., and Zeng, S. (2017). The regioselective glucuronidation of morphine by dimerized human UGT2B7, 1A1, 1A9 and their allelic variants. Acta Pharmacol. Sin. *38*, 1184–1194.

Yeh, S.Y. (1975). Urinary excretion of morphine and its metabolites in morphine-dependent subjects. J. Pharmacol. Exp. Ther. *192*, 201–210.

Yoshimura, H., Îda, S., Oguri, K., and Tsukamoto, H. (1973). Biochemical basis for analgesic activity of morphine-6-glucuronide—I: Penetration of morphine-6-glucuronide in the brain of rats. Biochem. Pharmacol. *22*, 1423–1430.

Footnotes

Financial support: This work was supported by a Foundation Grant from the Canadian Institute of Health Research (CIHR) awarded to PS (Grant no. FDN-148413), and by CIHR grant awarded to L.G. (Grant nos. MOP-123399 and MOP-136871). PS holds a Canada Research Chair in Neurophysiopharmacology of Chronic Pain. L.G. is the recipient of a Senior Salary support from the Fonds de la Recherche Québec–Santé.

Conflict of interest: The new chemical entities described herein are proprietary to Angiochem Inc. Michel Demeule, Anthony Régina, Gaoqiang Yang, and Alain Larocque were employees of Angiochem Inc., and are listed on company patent applications. Philippe Sarret has received research funding and consulting fees from Angiochem Inc. Louis Gendron has received research funding from Angiochem Inc.

FIGURE LEGENDS:

Scheme 1. A. Synthesis of (Morphine-PEG)$_3$-Angiopep-2 (3). **B.** Synthesis of (M6G)$_3$-Angiopep-2 (7).

Figure 1. Brain uptake of radioactive morphine, An2-morphine and An2-M6G measured by in situ brain perfusion. (**A**) Time course of brain uptake of [^{3}H]-morphine, [^{125}I]-An2-morphine and [^{125}I]-An2-M6G. Representation of the distribution volume (V_d) in brain homogenate. (**B**) Quantification of [^{3}H]-morphine, [^{125}I]-An2-morphine and [^{125}I]-An2-M6G in total brain, capillaries and parenchymal fractions after 2 minutes of perfusion. Data represent mean ± SEM (n= 3-4). ** $p < 0.01$, *** $p < 0.001$; two-way ANOVA test followed by Tukey's multiple comparison test.

Figure 2. Antinociceptive effects of intravenous morphine and An2-morphine in the tail flick assay. The antinociceptive effects of morphine and An2-morphine were evaluated by measuring the time to tail withdrawal in the tail-flick assay. Rats were treated i.v. with saline or with increasing doses of either morphine sulfate (MS) [0.3 mg/kg (n=10), 1 mg/kg (n=7) and 3 mg/kg (n=10)] (**A**) or An2-morphine [0.3 mg/kg (n=10), 1 mg/kg (n=10) and 3 mg/kg (n=9)] (**D**). For each dose, the percentage of the maximal possible effect (% MPE) was calculated for morphine and An2-morphine, as shown in panels **B** and **E**, respectively. The Area Under the Curve (AUC) representing the total drug exposure across time (i.e. 120 min) following administration of increasing doses of MS are represented in panel **C** while the AUC of equimolar doses of An2-morphine are shown in panel **F**. * $p < 0.05$, ** $p < 0.01$, **** $p < 0.0001$ compared to the saline group; one-way ANOVA followed by Dunnett's multiple comparisons test.

Figure 3. Antinociceptive effects of intravenous morphine-6-glucuronide (M6G) and An2-M6G in the tail-flick assay. The antinociceptive effects of (M6G) and An2-M6G were evaluated by measuring the time to tail withdrawal in the tail-flick assay. Rats were treated i.v. with saline or with increasing doses of either M6G [1.5 mg/kg (n=10), 3 mg/kg (n=7) and 4.5 mg/kg] (n=10) (**A**) or An2-M6G [1.2 mg/kg (n=6), 4 mg/kg (n=9), 8 mg/kg (n=5) and 12 mg/kg] (n=6) (**D**). For each dose, the percentage of the maximal possible effect (% MPE) was calculated for M6G and An2-M6G (panels **B** and **E)**. The AUC calculated for the whole period of time are represented in panels **C** and **F**. * $p < 0.05$, ** $p < 0.01$, **** $p < 0.0001$ compared to the saline group; one-way ANOVA followed by Dunnett's multiple comparisons test.

Figure 4. Antinociceptive effects of intravenous morphine, An2-morphine, morphine-6-glucuronide and An2-M6G in the hot-plate test. The antinociceptive effects of morphine (MS), An2-morphine, morphine-6-glucuronide (M6G) and An2-M6G were evaluated by measuring the paw licking behaviors of adult male CD1 mice in the thermal hot-plate assay. Mice were injected i.v. with saline, 10 mg/kg of MS or 30 mg/kg of An2-morphine (**A**) or saline, 1.5 mg/kg of morphine, 3 mg/kg of M6G and 6 mg/kg of An2-M6G (n=5 per group) (**D**). For each drug, the % MPE was calculated, as shown in panels **B** and **E**. The AUC following administration of equimolar doses of MS and An2-morphine are represented in panel **C** while the AUC of equimolar doses of MS, M6G and An2-M6G are shown in panel **F**. ** $p < 0.01$, *** $p < 0.001$ and **** $p < 0.0001$ compared to saline group; # $p < 0.05$ and # # # # $p < 0.0001$ compared to An2-M6G; one-way ANOVA test followed by Tukey's multiple comparison test.

Figure 5. Antinociceptive effects of subcutaneous morphine, An2-morphine, morphine-6-glucuronide and An2-M6G in the tail-flick assay. The antinociceptive effects of morphine (MS), An2-morphine, morphine-6-glucuronide (M6G) and An2-M6G were evaluated by

measuring the time to tail withdrawal in the tail flick assay. Rats were injected s.c. with saline, 5 mg/kg of MS or 20 mg/kg of An2-morphine (**A**) or saline, 3 mg/kg of morphine, 5 mg/kg of M6G and 12 mg/kg of An2-M6G (n=9-10 per condition) (**D**). For each drug, the % MPE was calculated, as shown in panels **B** and **E**. The AUC following administration of equimolar doses of MS and An2-morphine are represented in panel **C** while the AUC of equimolar doses of MS, M6G and An2-M6G are shown in panel **F**. ***$p < 0.001$ and ****$p < 0.0001$ compared to saline group; # $p < 0.05$ and # # # #$p < 0.0001$ compared to MS group; $$ $p < 0.01$; $$$ $p < 0.001$; one-way ANOVA test followed by Tukey's multiple comparison test. &: the baseline was used at 180 min to calculate the AUC of morphine group until 180 min.

JPET Fast Forward. Published on April 23, 2020 as DOI: 10.1124/jpet.119.263566
This article has not been copyedited and formatted. The final version may differ from this version.

Table 1. *In vivo* brain uptake of the compounds expressed in influx rate constant (K_{in}). # The M6G and glucose values used are from Wu *et al*. (1997b).

Compounds	Brain K_{in} (mL/s/g)	
	Experimental	Theoretical #
Glucose		$9.5x10^{-3}$
Morphine	$2.2x10^{-4}$	
An2-morphine	$2.7x10^{-3}$	
M6G		$2x10^{-5}$
An2-M6G	$8.8x10^{-3}$	

JPET Fast Forward. Published on April 23, 2020 as DOI: 10.1124/jpet.119.263566
This article has not been copyedited and formatted. The final version may differ from this version.

Table 2. Effect of morphine, An2-M6G and An2-morphine on the gastrointestinal tract motility. Saline, MS (1, 5 and 10 mg/kg), An2-M6G (4 and 20 mg/kg) and An2-morphine (20 mg/kg) were injected s.c. 30 min before force-feeding with a charcoal meal solution. The progression of the charcoal meal in the intestine was measured 1 hour after force-feeding. *$p < 0.05$, ***$p < 0.001$, ****$p < 0.0001$ compared to saline group; $^{\$}p < 0.05$ An2-M6G (20 mg/kg) compared to An2-morphine (20 mg/kg); Kruskal-Wallis nonparametric test followed by Dunn's multiple-comparison test.

Treatment	Saline	Morphine (MS)			An2-M6G		An2-morphine
n	10	10	10	10	10	10	10
Dose (mg/kg)		1	5	10	4	20	20
Equimolar MS					1	5	5.5
Progression of the charcoal meal in the intestine (% ± SEM)	73.4 ± 2.2	58 ± 2.7 *	49.7 ± 2.7 ***	28.6 ± 3.7 ****	61.5 ± 3.3	59.7 ± 3.1$^{\$}$	45.1 ± 5.1 ****

Scheme 1

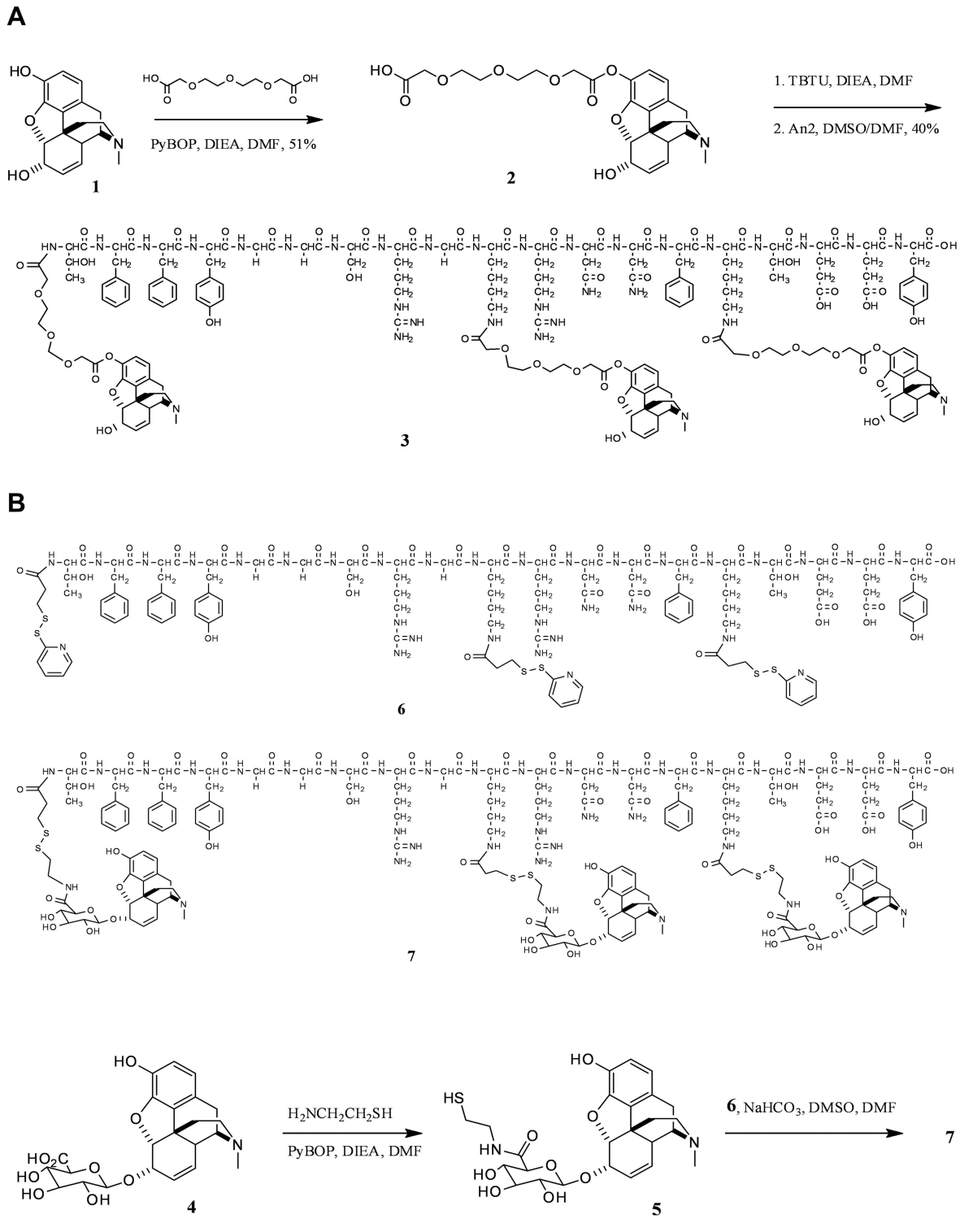
A
PyBOP, DIEA, DMF, 51%
1. TBTU, DIEA, DMF
2. An2, DMSO/DMF, 40%
1
2
3
B
6
7
$H_2NCH_2CH_2SH$
PyBOP, DIEA, DMF
6, $NaHCO_3$, DMSO, DMF
4
5
7

Figure 1

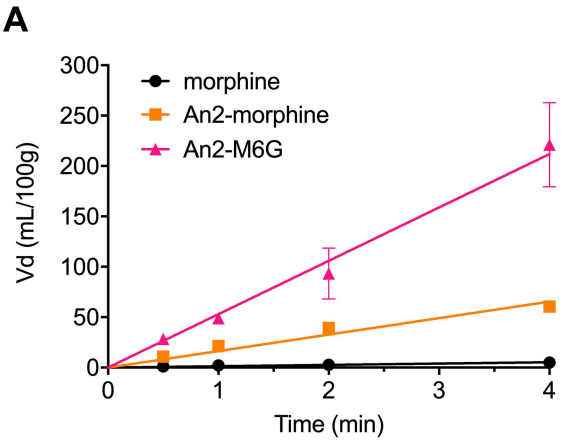
A
300
250
200
150
100
50
0
Vd (mL/100g)
morphine
An2-morphine
An2-M6G
0
1
2
3
4
Time (min)

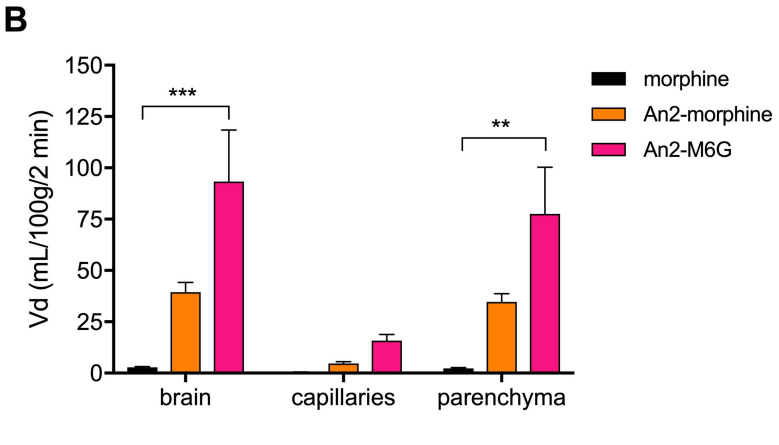
B
150
125
100
75
50
25
0
Vd (mL/100g/2 min)
***
**
morphine
An2-morphine
An2-M6G
brain
capillaries
parenchyma

Figure 2

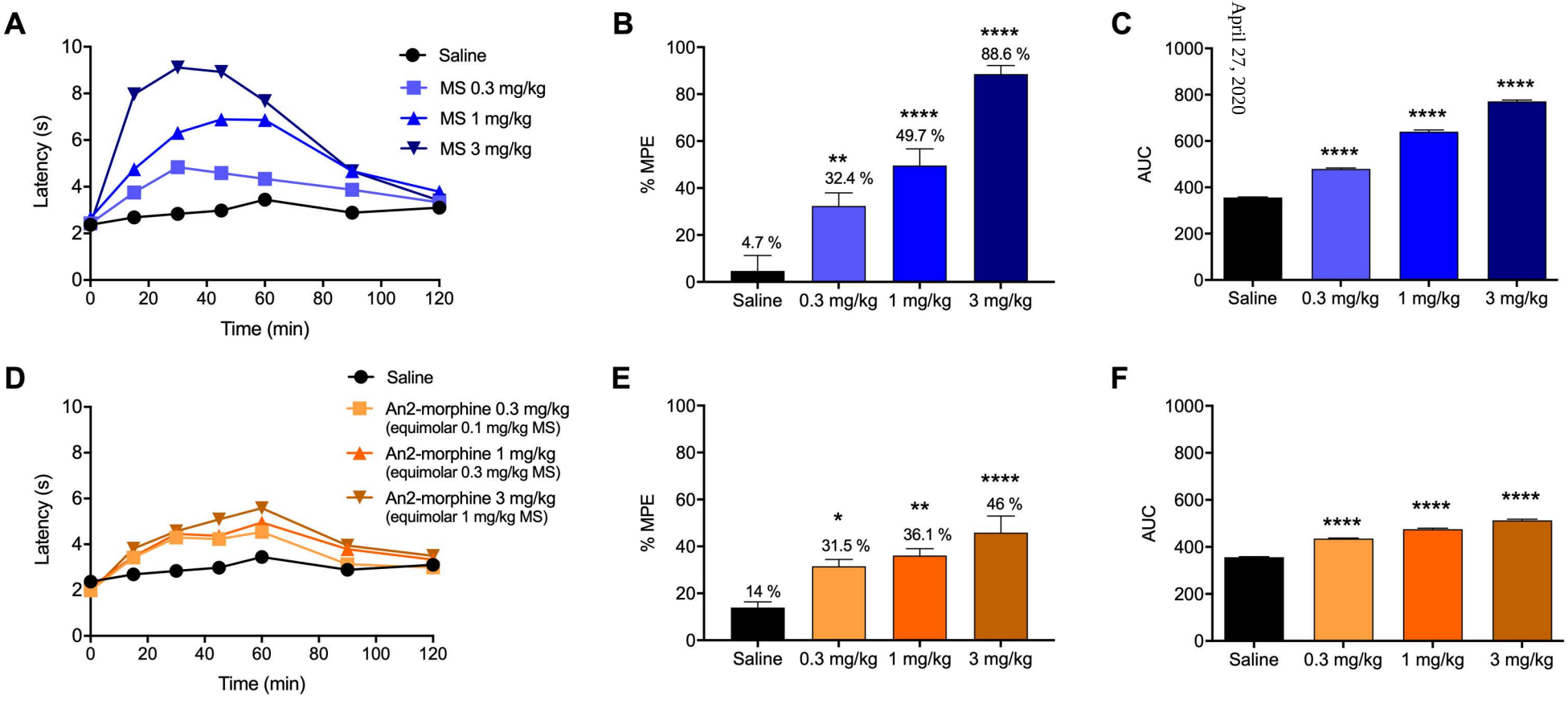

Figure 3

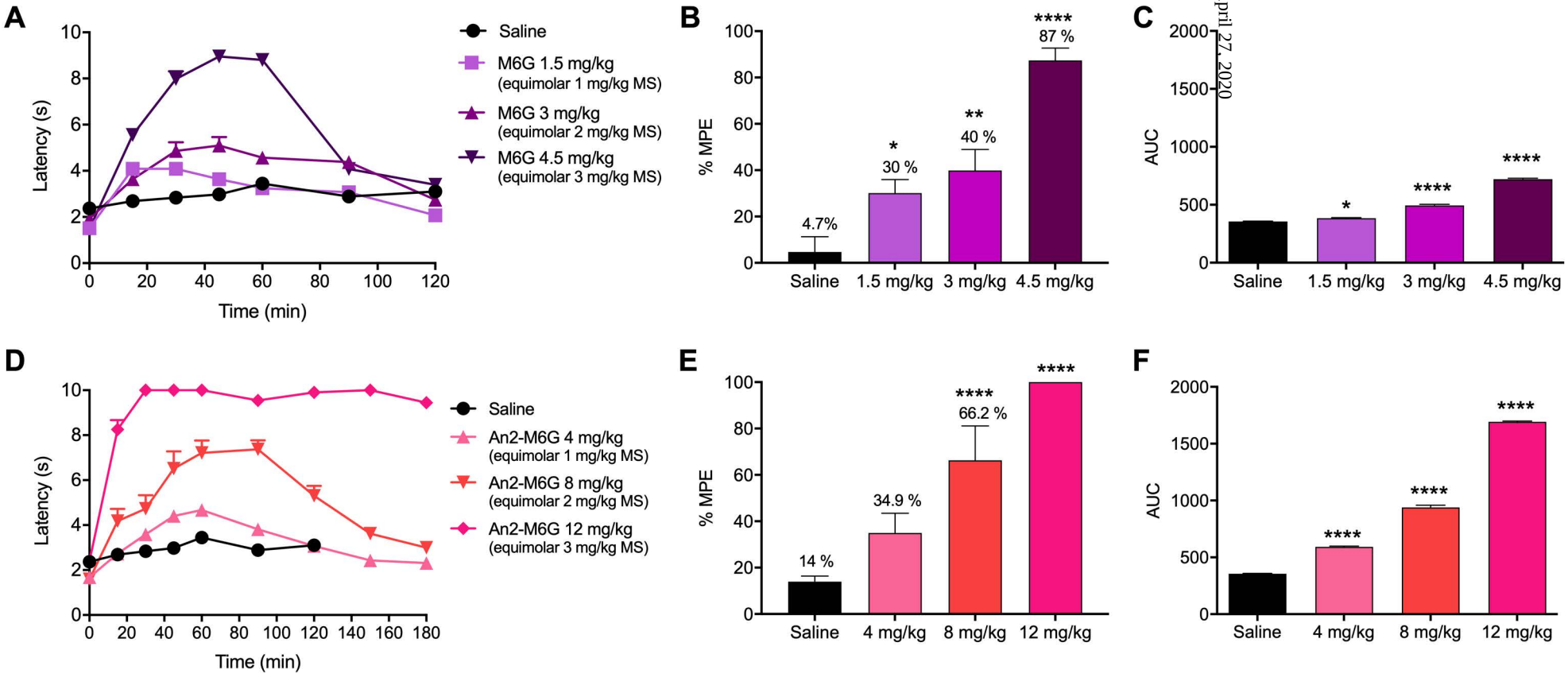

Figure 4

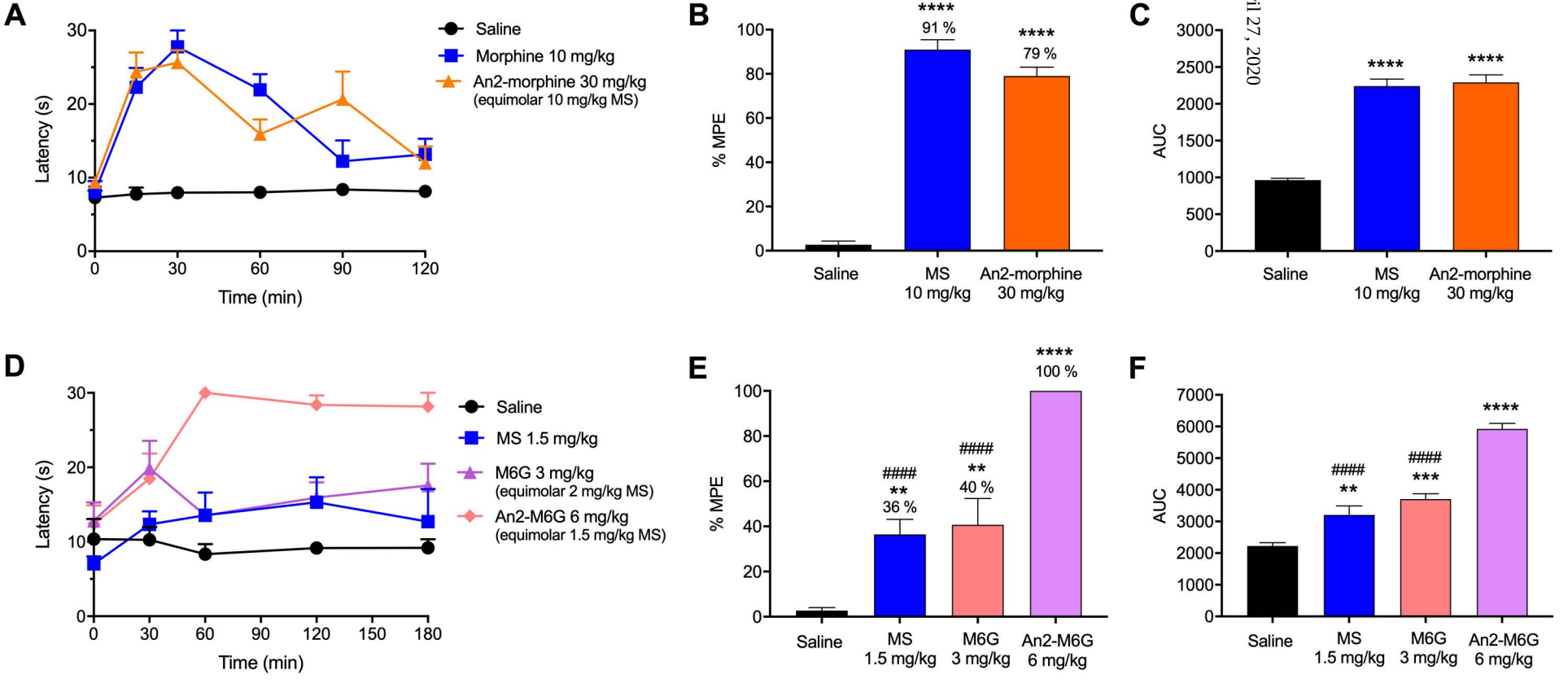

Figure 5